Particle Filter based Grid Synchronization with Voltage Unbalance and Frequency Variation in Smart Grid

Jiangcai Zhu[†], Zhiguo Shi[†,‡], Hao Liang[‡], Rongxing Lu[♯], and Xuemin (Sherman) Shen[‡]
[†]Department of Information and Electronic Engineering, Zhejiang University, Hangzhou 310027, China
[‡]Dept. ECE, University of Waterloo, Canada; [♯]School of EEE, Nanyang Technological University, Singapore.
Email: {1992_zjc, shizg}@zju.edu.cn; {h8liang, xshen}@bbcr.uwaterloo.ca; rxlu@ntu.edu.sg

***Abstract*—Computing the phase angle of a three-phase voltage signal in utility grid is critical for the synchronization of smart grid. Only if the phase angle is accurately estimated, the energy transfer between the distributed power generators and the utility grid can be properly controlled. In this paper, we propose a particle filter (PF) based scheme to estimate the phase angle of the utility grid in the presence of voltage unbalance and frequency variation in the $\alpha\beta$ stationary reference frame where the positive and negative sequences of the input three-phase signal are separated by Clarke transformation. For the filter algorithm, the traditional SIR filter is customized for the grid synchronization problem by exploiting the feature of the grid state system dynamics and incorporating the deterministic resampling. Extensive simulations have been conducted to verify the effectiveness and efficiency of the proposed PF-based synchronization scheme. It is shown that the proposed PF-based scheme outperforms the traditional EKF-based scheme in terms of both estimation accuracy and convergence time, when both the voltage imbalance and frequency variation are exerted.**

Keywords* — *Extended Kalman filter, grid synchronization, particle filter, phase angle estimation.

I. Introduction

With more renewable energy source based distributed power generation systems (DPGS) being connected to utility grid, the necessity for accurate and efficient grid synchronization is ever-growing [1]. The main task of grid synchronization is to compute the phase angle of the three-phase voltage signal in utility grid. Without grid synchronization, DPGS can not be properly controlled and their connection to the utility network may lead to grid instability. Moreover, when several DPGS transmit their power to the buses in utility grid, the transform efficiency can be improved by achieving perfect grid synchronization in each distributed generator (DG). The reason lies in that, the transmitted active power is proportional to the phase difference between the bus of a DG and the utility grid [2]. Only when grid synchronization is achieved, a DG can adjust its phase to maximize its transmission efficiency.

Grid synchronization is a very challenge task. For a three-phase voltage signal in the presence of voltage unbalance, it is composed of positive, negative and zero sequences. In grid synchronization, the positive sequence of signal has to be identified to obtain the phase angle of the ideal signal. It is very challenging because a double frequency component will be introduced due to the existence of negative sequence [3]. Further more, when the frequency variation in real-world utility grid is taken into consideration, the task becomes even more difficult.

In traditional power grid, phasor measurement units (PMUs) are deployed to measure the phase of three-phase voltage / current signals [4]. They play an important role in power system monitoring, protection and control. In North America, about 500 networked PMUs have been deployed. However, for small scale DGs, it is not proper to deploy the traditional PMUs to measure the voltage phase due to the high hardware complexity and high cost of PMUs [5], [6]. One solution for the DGs is to let the deployed PMUs help to process the signal by using enhanced transmission technology in smart grid, but the computation burden for the PMUs will become very heavy and the communication overhead is significant [7], [8]. Thus, designing a "miniPMU" which can measure the voltage signal phase with low hardware complexity and cost in local DGs motivates the study of this work. In this miniPMU, analog signals are first converted to digital signals, and then digital filters are designed to estimate the phase of the positive sequence signal.

One of the key issues in designing this kind of miniPMU is the filter algorithm for grid synchronization utilized in the system. In this paper, we propose a synchronization scheme based on particle filter (PF), which is a state-of-the-art solution for non-linear and non-Gaussian systems [9], [10]. Since the state dynamics of power signal can be represented by a highly non-linear system, the estimation performance of state variables by using a PF is expected to have better performance than that of the extended Kalman filter (EKF) [11]. The main contribution of this work is two fold. First, after formulating the grid synchronization problem into a Bayesian filtering framework, we design a PF-based scheme which exploits the feature of the utility grid system dynamics for state variables estimation and employs a threshold-based resampling for real-time performance improvement. Second, we conduct extensive simulations to validate the effectiveness of the proposed grid synchronization scheme and compare its performance with the EKF-based results.

The remainder of this paper is organized as follows. In Section II, we discuss the related work. In Section III, we describe

the problem formulation of grid synchronization, and present the design of the PF-based synchronization scheme under the Bayesian framework. Then, we conduct extensive simulation and make comparison between the proposed scheme with the EKF-based scheme in Section IV. Finally, we conclude this paper in Section V.

II. Related Work

The problem of detecting the phase angle of grid voltage signal with voltage unbalance has been studied in the last several years and many methods has been proposed [11]–[14]. Among them, the voltage zero-crossing method is the most simple and easy one. However, disturbances in the input signal, such as voltage unbalance and harmonics, degrade the accuracy of the method. To address this problem, filtering techniques including low-pass filters and recursive weighted least-square estimation have been employed for grid synchronization [12], to achieve better estimation accuracy than the zero-crossing methods and get fast transient response, even in the presence of some distorted conditions. In addition, some phase-locked loop (PLL) based phase estimation techniques are proposed in [14], which are able to reject harmonics, voltage unbalance, and other kinds of disturbances. However, these methods have rather complex hardware structure and are not suitable to be implemented in the miniPMUs.

In [11], a nonlinear synchronization method based on EKF is proposed. The input three-phase signal is transformed to the $\alpha\beta$ stationary reference frame, and the system state equation and measurement equation are established. After the system models are available, an EKF is used to estimate the state variable for obtaining the phase angle of the grid voltage signal in the presence of voltage unbalance and frequency variation. It has a comparatively much simpler structure and is suitable for miniPMU applications. However, we notice that the system state equation is highly nonlinear, and EKF utilizes only the first order Taylor expansion of the nonlinear model. Thus, there are rooms to improve the estimation performance. Since PF is a kind of Sequential Monte Carlo (SMC) approach which is more suitable for solving nonlinear and/or non-Gaussian problems than the traditional extended Kalman filter (EKF), in this paper we design a PF-based scheme to solve this problem.

III. Particle Filter based Scheme for Grid Synchronization

In this section, we describe the problem formulation of grid synchronization under the Bayesian framework, present the detailed design of the PF for state variables estimation, and show how to use the estimated state variables to determine the phase angle of the positive sequence voltage signal.

A. Problem Formulation

The main objective of grid synchronization is to obtain the phase angle of the positive sequence from the three-phase voltage signal. The phase angle is then used to synchronize the on/off state of power devices, calculate and control the flow of active/reactive power, adjust the phase angle of DGs to achieve maximum transform efficiency from DGs to buses in utility grid.

As shown in Fig. 1, the grid synchronization process consists of three stages [11]: 1) Reference Frame Transformation: use Clarke transformation to transform the three-phase input signal into the $\alpha\beta$ domain; 2) Variable Tracking: estimate the grid state variables with respect to the in-phase sinusoidal signals, quadrature sinusoidal signals, and grid frequency; and 3) Phase Angle Computation: after the grid state variables are obtained, compute the phase angle of the positive sequence based on their internal relationships.

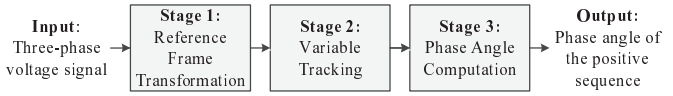

Fig. 1. Three steps of grid synchronization.

The input three-phase voltage signal of a utility grid can be described by

$$\begin{aligned} v_a(n) &= V_a \cos(n\omega + \varphi_a) + e_a(n) \\ v_b(n) &= V_b \cos(n\omega + \varphi_b) + e_b(n) \\ v_c(n) &= V_c \cos(n\omega + \varphi_c) + e_c(n) \end{aligned} \tag{1}$$

where n ($n = 0, 1, 2, \ldots$) is the time index, and V_i and φ_i denote the amplitude and initial phase angle of signal i ($i = a, b, c$). The angular frequency ω of the grid is defined as $\omega = 2\pi f/f_s$, where f_s is the sampling frequency and f is the grid frequency with its nominal value f_0 equalling 50 Hz or 60 Hz in most countries. $e(n) = [e_a(n), e_b(n), e_c(n)]^T$ is the additive noise which is assumed to be a zero-mean Gaussian random vector. The noise vectors at different time indexes are uncorrelated, i.e., $E[e(n)e(m)^T] = 0$ for $n \neq m$. Considering the presence of voltage unbalance and frequency variation, the values of V_a, V_b and V_c may not be the same, φ_a, φ_b and φ_c may not obey the relationship that $\varphi_b = \varphi_a - 2\pi/3$ and $\varphi_c = \varphi_a + 2\pi/3$, and f may have very small fluctuation around its nominal value f_0.

When the input signal in (1) is transformed into the $\alpha\beta$ stationary reference frame, it becomes:

$$[v_\alpha(n), v_\beta(n)]^T = \mathbf{T}[v_a(n), v_b(n), v_c(n)]^T \tag{2}$$

where $\mathbf{T}$ is the Clarke transformation defined as

$$\mathbf{T} = \frac{2}{3}\begin{bmatrix} 1 & -\frac{1}{2} & -\frac{1}{2} \\ 0 & \frac{\sqrt{3}}{2} & -\frac{\sqrt{3}}{2} \end{bmatrix}. \tag{3}$$

Then, the signal defined in (2) can be rewritten as

$$v_\alpha(n) \triangleq V_\alpha \cos(n\omega + \varphi_\alpha) + e_\alpha(n) \tag{4}$$

$$v_\beta(n) \triangleq V_\beta \cos(n\omega + \varphi_\beta) + e_\beta(n) \tag{5}$$

where V_i and φ_i denote the amplitude and initial phase angle of signal i ($i = \alpha, \beta$), and $e_\alpha(n)$ and $e_\beta(n)$ are noises for the α component and β component, respectively.

To establish the system dynamic model, five state variables, including the in-phase and quadrature signals of both $v_\alpha(n)$ and $v_\beta(n)$, as well as the grid frequency, are defined as [15]:

$$\begin{aligned} x_{1_n} &= V_\alpha \cos(n\omega + \varphi_\alpha) \\ x_{2_n} &= V_\alpha \sin(n\omega + \varphi_\alpha) \\ x_{3_n} &= V_\beta \cos(n\omega + \varphi_\beta) \\ x_{4_n} &= V_\beta \sin(n\omega + \varphi_\beta) \\ x_{5_n} &= \omega. \end{aligned} \tag{6}$$

Accordingly, the state equation can be formulated as:

$$\begin{aligned} \mathbf{X}_{n+1} &= f(\mathbf{X}_n) \\ &= \begin{bmatrix} x_{1_n}\cos(x_{5_n}) - x_{2_n}\sin(x_{5_n}) \\ x_{1_n}\sin(x_{5_n}) + x_{2_n}\cos(x_{5_n}) \\ x_{3_n}\cos(x_{5_n}) - x_{4_n}\sin(x_{5_n}) \\ x_{3_n}\sin(x_{5_n}) + x_{4_n}\cos(x_{5_n}) \\ (1-\epsilon)x_{5_n} \end{bmatrix} + \mathbf{e}_{w_n} \end{aligned} \tag{7}$$

where the state vector is $\mathbf{X}_n = [x_{1_n}, x_{2_n}, x_{3_n}, x_{4_n}, x_{5_n}]^T$, and $\mathbf{e}_{w_n}$ is the process noise which can be modeled as a Gaussian distributed random variable with zero-mean and covariance matrix $\mathbf{Q}$. In (7), $f(\cdot)$ is a system transition function which contains both sinusoid and cosine functions and is highly nonlinear. The parameter ϵ is introduced to represent the slowly time-varying characteristic of the grid frequency.

The measurement equation is given by

$$\mathbf{Z}_n = h(\mathbf{X}_n) = \mathbf{H}\mathbf{X}_n + \mathbf{e}_{v_n} \tag{8}$$

where $\mathbf{e}_{v_n}$ is the measurement noise and is modeled as a Gaussian distributed random variable with zero-mean and covariance matrix $\mathbf{R}$. In (8), $h(\cdot)$ is the measurement function, $\mathbf{Z}_n$ is the observation vector represented as $\mathbf{Z}_n = [v_\alpha(n), v_\beta(n)]^T$, and $\mathbf{H}$ is defined as

$$\mathbf{H} = \begin{bmatrix} 1 & 0 & 0 & 0 & 0 \\ 0 & 0 & 1 & 0 & 0 \end{bmatrix}. \tag{9}$$

B. PF Design for Grid State Estimation

In grid synchronization, the most critical stage is the grid state variable estimation. Once the state variables are estimated, the phase angle can be determined according to their internal relationships. From (7), it can be seen that the system dynamics contains highly nonlinear equations. Thus, different from the existing EKF-based scheme [11], in this paper, a properly designed PF is employed to estimate the state variables $\mathbf{X}_{1:n}$ from the observation vectors $\mathbf{Z}_{1:n}$. The possible advantage of particle filtering over the EKF-based scheme is that it does not involve linearization around current state estimation, but uses discrete particles to approximate the posterior probability density function (PDF). In this way, PF may yield the estimation performance improvement in comparison with the EKF-based scheme.

The main idea of PF is to represent the required posterior PDF $p(\mathbf{X}_n|\mathbf{Z}_{1:n})$ at time index n by a set of random samples $\{\mathbf{X}_n^j\}_{j=1}^N$ (N is the number of particles used) with associated weights (particle probability) $\{w_n^j\}_{j=1}^N$ and to compute the estimation based on these samples and weights as follows [16]

$$p(\mathbf{X}_n|\mathbf{Z}_{1:n}) \approx \sum_{i=1}^{N} w_n^j \delta(\mathbf{X}_n - \mathbf{X}_n^j). \tag{10}$$

If the particles are drawn in proper positions and the number of samples is large enough, these samples can very closely represent the true posterior PDF.

Generally, after initialization, a PF contains the following three steps of processing iteratively [16]:

1) **sampling**: draw a set of particles $\mathbf{X}_n^j \sim \pi(\mathbf{X}_n|\mathbf{X}_{n-1}^j)$ for $j = 1, ..., N$, where $\pi(\mathbf{X}_n|\mathbf{X}_{n-1}^j)$ is the proposal important density. In this paper, for simplicity, we set $\pi(\mathbf{X}_n|\mathbf{X}_{n-1}^j) = p(\mathbf{X}_n|\mathbf{X}_{n-1}^j)$
2) **weight calculating**: for each particle $\mathbf{X}_n^j$, calculate its weight w_n^j according to the measurement $\mathbf{Z}_n$ and its weight in previous time index by:

$$w_n^j = \tilde{w}_{n-1}^j \frac{p(\mathbf{Z}_n|\mathbf{X}_n^j)p(\mathbf{X}_n^j|\mathbf{X}_{n-1}^j)}{\pi(\mathbf{X}_n|\mathbf{X}_{n-1}^j)} \tag{11}$$

3) **resampling**: Based on the available particles $\mathbf{X}_n^j$ and their weights w_n^j, use a selected resampling algorithm to draw new particles $\mathbf{X}_n^j$ and assign weights w_n^j to each of them.

In this paper, to achieve better estimation performance, we design a PF customized for the estimation of grid state as shown in Algorithm 1. The basic filter structure is mainly inherited from the traditional SIR particle filter [16]. The customization to the SIR mainly contains two parts: first, in the sampling step, after sampling a particle from its previous state, we will check its validity to see whether the particle generation need to be repeated, as shown Algorithm 1; second, in the resampling step, we adopt the threshold-based resampling [10] for possible enhancement of parallel processing to improve the real-time performance. In addition, when calculating the particle weight, we add a very small value of 10^{-100} in order to prevent the weight from being zero to achieve better algorithm convergency.

The particle state validity checking is based on the fact that, unlike those general state tracking and estimation problems, for the state variables in (7), each of them has a corresponding maximum and minimum value, which can be used in the sampling steps. When a particle is generated, each state variable of it will be compared with the corresponding maximum and minimum values (value boundary). If any variable of the particle is out of the value boundary, the particle is regarded as out of possible value boundary and will be sampled again. This customization eliminates the particles that contributes nothing to the correct representation of posterior PDF of grid state and makes the estimation algorithm more efficient in terms of computation and more effective in terms of estimation performance.

Resampling is a critical step to eliminate low weight particles and multiply the particles with higher weight to increase the estimation accuracy. Several resampling schemes have

Algorithm 1 $[\{\mathbf{X}_n^j, w_n^j\}_{j=1}^N] = PF[\{\mathbf{X}_{n-1}^j, w_{n-1}^j\}_{j=1}^N]$

BEGIN:

1) Loop Initialization: $n = 0$

1: **for** $j = 1, 2, ..., N$ **do**
2: Draw $\mathbf{x}_0^j$ using the procedure proposed in [17];
3: Assign particle weight $w_n^j = 1/N$;
4: Initialize threshold: $T < 1/N$
5: **end for**

2) Main Loop:

for k=1,2,... **do**
for $j = 1 : N$ **do**
Draw $\mathbf{X}_n^j \sim \pi(\mathbf{X}_n|\mathbf{X}_{n-1}^j) = p(\mathbf{X}_n|\mathbf{X}_{n-1}^j)$
while ($\mathbf{X}_n^j$ out of the possible value boundary) **do**
Re-Draw $\mathbf{X}_n^j$;
end while
Calculate $w_n^j = \frac{1}{2\pi\sqrt{\mathbf{R}(1,1)\mathbf{R}(2,2)}}(\frac{(\mathbf{H}\mathbf{X}_n^j(1)-\mathbf{Z}_n(1))^2}{\sqrt{\mathbf{R}(1,1)}}$
$+\frac{(\mathbf{H}\mathbf{X}_n^j(2)-\mathbf{Z}_n(2))^2}{\sqrt{\mathbf{R}(2,2)}}) + 10^{-100}$
end for
Calculate total weight: $t = \text{SUM}[\{w_n^j\}_{j=1}^N]$
for $j = 1 : N$ **do**
Normalize: $w_n^j = t^{-1}w_n^j$
end for
$i = 0$
for $j = 1 : N$ **do**
if $w_n^j > T$ **then**
$i = i + 1$
$\hat{\mathbf{X}}_n^i = \mathbf{X}_n^j$
end if
end for
$r = 1$
for $j = 1 : N$ **do**
Assign sample: $\mathbf{X}_n^j = \hat{\mathbf{X}}_n^r$
Assign weight: $w_n^j = 1/N$
$r = \text{mod}(r, i) + 1$
end for
end for

END

been proposed in literatures, such as systematic resampling (SR), residual SR, and some kinds of deterministic resampling. In this paper, we adopt the threshold-based resampling proposed in [10], where the weights of each particle are compared with a threshold T. For the particles with weights that are greater than T, they are called substantial particles and will be retained, otherwise, they are called negligible particles and will be discarded. The threshold-based resampling can improve the real-time performance of PF because each particle can be resampled as soon as its weight is obtained, i.e., the sequential nature of the traditional SR or RSR can be overcome. From the estimation performance point of view, it is shown in [10] that with a properly selected threshold T, the sampling can achieve the same level of estimation performance as the traditional SR and RSR. Following the design guide in [10], in this paper, the threshold is set as $\frac{1}{10N}$.

C. Phase Angle Computation

Once the state vector $\mathbf{X}$ is estimated at each time index n, the phase angle of the positive sequence can be computed by the following equations:

$$\begin{aligned}
\hat{V}_\alpha \sin(\hat{\varphi}_\alpha) =& x_{2_n} \cos((n-1)x_{5_n} \\
& - x_{1_n} \sin((n-1)x_{5_n} \\
\hat{V}_\alpha \cos(\hat{\varphi}_\alpha) =& x_{2_n} \sin((n-1)x_{5_n} \\
& + x_{1_n} \cos((n-1)x_{5_n} \\
\hat{V}_\beta \sin(\hat{\varphi}_\beta) =& x_{4_n} \cos((n-1)x_{5_n} \\
& - x_{3_n} \sin((n-1)x_{5_n} \\
\hat{V}_\beta \cos(\hat{\varphi}_\beta) =& x_{4_n} \sin((n-1)x_{5_n} \\
& + x_{3_n} \cos((n-1)x_{5_n}
\end{aligned} \tag{12}$$

$$\hat{\varphi}_p = \arctan \frac{\hat{V}_\alpha \sin \hat{\varphi}_\alpha + \hat{V}_\beta \cos \hat{\varphi}_\beta}{\hat{V}_\alpha \cos \hat{\varphi}_\alpha - \hat{V}_\beta \sin \hat{\varphi}_\beta} \tag{13}$$

$$\hat{\theta}_p(n) = (n-1)x_{5_n} + \hat{\varphi}_p. \tag{14}$$

IV. Simulation Results and Discussion

In this section, we describe the simulation set up for the proposed PF-based grid synchronization scheme, and then show simulation results of the estimation of the grid state and the consequent grid phase. The results are compared with the EKF-base scheme.

A. Simulation Setup

In the simulation, for the system model, the amplitudes and initial phase angles of the three-phase voltage signal are set to 1.0, 1.2, 0.8 and 0, $-\frac{\pi}{3}$, $\frac{2\pi}{3}$, respectively, to model the voltage unbalance. The process noise covariance is $\mathbf{Q} = \begin{bmatrix} \sigma^2\mathbf{I}_{4\times4} & \mathbf{0} \\ \mathbf{0} & q \end{bmatrix}$, where σ is set to $10^{-3}, 10^{-4}$ and 10^{-5} for comparative study, $\mathbf{I}_{4\times4}$ is the 4×4 identity matrix and $q = 10^{-7}$. The value of parameter ϵ is 10^{-16}. The measurement noise covariance is $\mathbf{R} = r\mathbf{I}_{2\times2}$, where r is set to $\{10^{-n}, n = 1, 2, \ldots, 10\}$ and $\mathbf{I}_{2\times2}$ is the 2×2 identity matrix. The sampling frequency f_s ($f_s = \frac{1}{T}$) is chosen as 1200 Hz and the nominal fundamental frequency f_0 is 60 Hz. The frequency is simulated to change from about 60 Hz to 61 Hz to testify the effectiveness of the proposed scheme to frequency variation.

For the PF, the number of particle is set as 300. To compare the performance with the EKF-based scheme in [11], the EKF-based scheme is also simulated. The estimation error covariance $\mathbf{P}$ used in EKF design is $\frac{10^{-4}}{2}\mathbf{I}_{5\times5}$ and $\mathbf{I}_{5\times5}$ is the 5×5 identity matrix.

B. Grid State Estimation

To show the estimation performance of the grid state, the root mean square error (RMSE) is used as the performance metric and defined as:

$$RMSE = \sqrt{\frac{1}{L}\sum_{n=1}^{L}\frac{1}{N_{MC}}\sum_{i=1}^{N_{MC}}(\hat{s}_n^i - s_n^{true})^2} \tag{15}$$

where L is the total number of simulation time steps, N_{MC} is the number of Monte Carlo simulations performed , $\hat{s}_n^i$ is the filter variable estimation at time index n in the $i-$th Monte Carlo run, and s_n^{true} is the true variable at time index n.

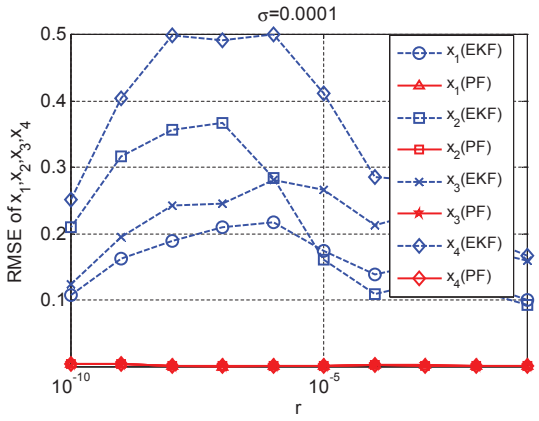

(a) RMSE of x_1, x_2, x_3, x_4.

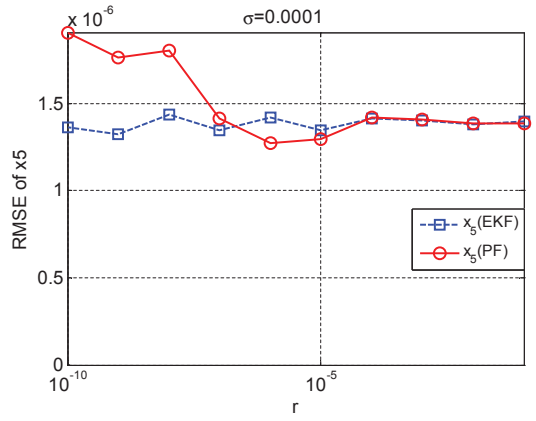

(b) RMSE of x_5.

Fig. 2. Root Mean Square Error (RMSE) of state variables.

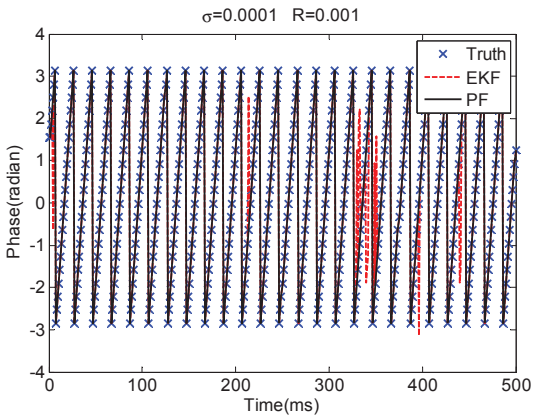

(a) Phase angle estimation in a single simulation.

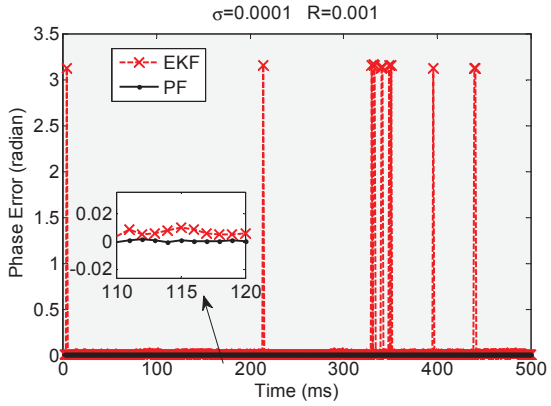

(b) Phase angle estimation error in a single simulation.

Fig. 3. Simulated phase angle estimation.

Fig. 2 shows the RMSE of the five state variables for both the EKF- and PF-based schemes for grid state estimation when $N_{MC} = 1000$, $L = 500$, $\sigma = 0.0001$, and r changes from 10^{-10} to 10^{-1}. For the first four states, the estimation of the PF is always much better than that of the EKF. For the last parameter, namely the frequency ω, the estimation of the PF is a little bit worse than that of the EKF when r is very very small as of below 10^{-7}. Note that in Fig. 2(b), since the errors of x_5 for both schemes are of 10^{-6} order of magnitude, it can be regarded as no performance gap. Thus, the PF outperforms the EKF in terms of estimation performance.

C. Phase Estimation Results

From the grid state variables, we can obtain the grid phase estimation. Fig. 3 shows the results of one round of simulation with $\sigma = 10^{-4}$ and $r = 10^{-3}$ to illustrate the convergence of the PF to the true phase angle of the grid. Estimation performance is compared with that of the EKF-based scheme. From Fig. 3(a), it can be seen that the PF-based scheme can always estimate the phase angle accurately, but the EKF-based scheme will have some obvious estimation errors in some time indexes. The performance difference can be observed in a more clear way from Fig. 3(b), where the absolute phase angle estimation errors defined as

$$e_{phase} = |\theta_{est} - \theta_{true}|, \tag{16}$$

with θ_{est} denoting the estimated phase and θ_{true} denoting the true phase, are shown. It is clear that the PF-based scheme is more accurate than the EKF-based scheme.

To further demonstrate the effectiveness of the proposed PF-based scheme, Fig. 4 shows the RMSE of the phase estimation for both the PF-based scheme and the EKF-based scheme in different conditions. Three different values of σ and ten different values of r are studied in our simulations. The results are averaged over 1000 Monte Carlo simulation runs. It can be seen that the RMSE of the phase angle obtained from the PF-based scheme is always smaller than 0.2 while that from the EKF-based scheme is much larger. Thus, the performance of the PF-based scheme is far superior to that of the EKF-based scheme.

To show the effectiveness of the proposed PF-based scheme in the presence of frequency variation, Fig. 5 plots process of estimating the frequency f over time when the frequency f_0 change from about 60 Hz to 61 Hz. It can be seen that, although the estimations of both the PF-based scheme and the EKF-based scheme fluctuate around the ground truth, both of them succeed in tracking the frequency change. For

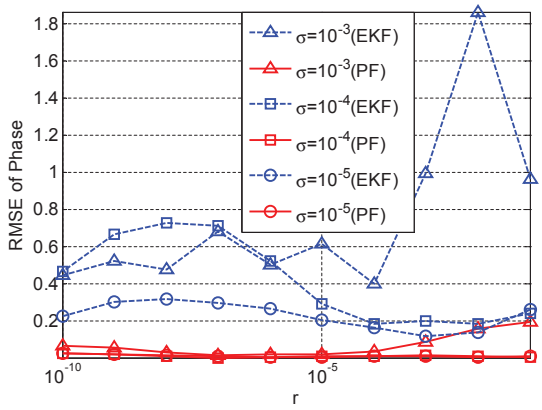

Fig. 4. RMSE of phase in different conditions.

comparison, we can see that the the estimated grid voltage frequency converges to the actual frequency much faster than that from the EKF estimator. This is because that the EKF is very sensitive to the initial states. Mathematical calculation from simulation results show that, the RMSE of phase estimation from the EKF-based scheme is 0.65989, while that from the PF-based scheme is 0.28105. This indicates that the performance of the PF-based scheme is superior to the EKF-based scheme when the frequency variation is exerted.

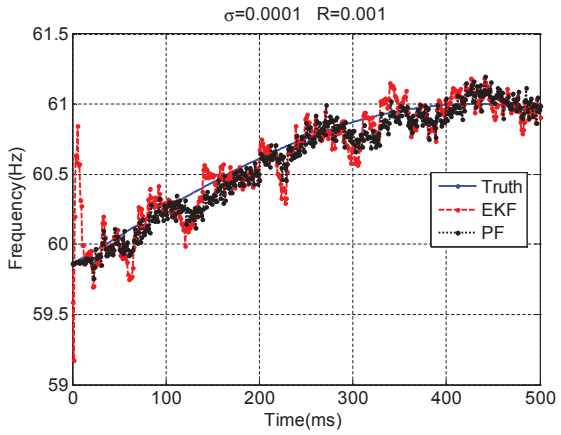

Fig. 5. Frequency estimates in a single simulation run.

V. Conclusion

In this paper, we have proposed a PF-based grid synchronization scheme for DGs to estimate the phase angle of grid voltage signal in smart grid. The traditional SIR filter is customized by exploiting the feature of the grid state system dynamic and incorporating the deterministic resampling. Extensive simulations have been conducted and the results demonstrate that, for both the grid state estimation and grid phase angle estimation, the PF-based scheme outperforms the EKF-based scheme in terms of the estimation accuracy and convergence time. In addition, the proposed PF-based scheme is effective when both the voltage imbalance and frequency variation are exerted. The whole processing can be implemented in a low cost microprocessor and this makes it possible to design a miniPMU in each small scale DG deployed in smart grid network.

Acknowledgment

This work was supported in part by NSFC (No. 61171149), the Fundamental Research Funds for the Chinese Central Universities (No. 2013xzzx008-2), and ORF-RE, Ontario, Canada.

References

[1] F. Blaabjerg, R. Teodorescu, M. Liserre, and A. V. Timbus, "Overview of control and grid synchronization for distributed power generation systems," *IEEE Transactions on Industrial Electronics*, vol. 53, no. 5, pp. 1398–1409, 2006.

[2] Y. Huang, M. Esmalifalak, H. Nguyen, R. Zheng, Z. Han, H. Li, and L. Song, "Bad data injection in smart grid: attack and defense mechanisms," *IEEE Communications Magazine*, vol. 51, no. 1, pp. 27–33, 2013.

[3] R. A. Flores, I. Y. Gu, and M. H. Bollen, "Positive and negative sequence estimation for unbalanced voltage dips," in *Proc. of 2003 IEEE Power Engineering Society General Meeting*, vol. 4. IEEE, 2003.

[4] F. Ding and C. Booth, "Applications of pmus in power distribution network with distributed generation," in *Proc. of the 46th International Universities' Power Engineering Conference*. IEEE, 2011, pp. 1–5.

[5] H. Liang, B. J. Choi, W. Zhuang, X. Shen, A. Awad, and A. Abdr, "Multiagent coordination in microgrids via wireless networks," *IEEE Wireless Communications*, vol. 19, no. 3, pp. 14–22, 2012.

[6] R. Lu, X. Liang, X. Li, X. Lin, and X. Shen, "Eppa: An efficient and privacy-preserving aggregation scheme for secure smart grid communications," *IEEE Transactions on Parallel and Distributed Systems*, vol. 23, no. 9, pp. 1621–1631, 2012.

[7] H. Liang, B. J. Choi, W. Zhuang, and X. Shen, "Stability enhancement of decentralized inverter control through wireless communications in microgrids," *IEEE Transactions on Smart Grid*, vol. 4, no. 1, pp. 321–331, 2013.

[8] R. Deng, J. Chen, X. Cao, Y. Zhang, S. Maharjan, and S. Gjessing, "Sensing-performance tradeoff in cognitive radio enabled smart grid," *IEEE Transactions on Smart Grid*, vol. 4, no. 1, pp. 302–310, 2013.

[9] Z. Shi, S. Hong, and K. Chen, "Experimental study on tracking the state of analog chua's circuit with particle filter for chaos synchronization," *Physics Letters A*, vol. 372, no. 34, pp. 5575–5580, 2008.

[10] S. Hong, Z. Shi, J. Chen, and K. Chen, "A low-power memory-efficient resampling architecture for particle filters," *Circuits, Systems, and Signal Processing*, vol. 29, no. 1, pp. 155–167, 2010.

[11] M. Sun and Z. Sahinoglu, "Extended kalman filter based grid synchronization in the presence of voltage unbalance for smart grid," in *Proc. 2011 IEEE PES Innovative Smart Grid Technologies*. IEEE, 2011, pp. 1–4.

[12] Z. Ma, H. Li, H. An, W. Wang, and J. Quan, "Algorithm of variable transition bandwidth fir filters with weighted-least-square method," in *Proc. 2nd International Conference on Computer Engineering and Technology*, vol. 7. IEEE, 2010, pp. V7–321.

[13] S.-K. Chung, "A phase tracking system for three phase utility interface inverters," *IEEE Transactions on Power Electronics*, vol. 15, no. 3, pp. 431–438, 2000.

[14] J. Akre, J. Juillard, D. Galayko, and E. Colinet, "Synchronization analysis of networks of self-sampled all-digital phase-locked loops," *IEEE Transactions on Circuits and Systems I*, vol. 59, no. 4, pp. 708–720, 2012.

[15] S. Bittanti and S. M. Savaresi, "On the parametrization and design of an extended kalman filter frequency tracker," *IEEE Transactions on Automatic Control*, vol. 45, no. 9, pp. 1718–1724, 2000.

[16] M. S. Arulampalam, S. Maskell, N. Gordon, and T. Clapp, "A tutorial on particle filters for online nonlinear/non-gaussian bayesian tracking," *IEEE Transactions on Signal Processing*, vol. 50, no. 2, pp. 174–188, 2002.

[17] Z. Shi, S. Hong, J. Chen, K. Chen, and Y. Sun, "Particle filter-based synchronization of chaotic colpitts circuits combating awgn channel distortion," *Circuits, Systems, and Signal Processing*, vol. 27, pp. 833–845, 2008.